Supporting Information

Di Modugno et al. 10.1073/pnas.1214394109

SI Materials and Methods

Cloning and Sequencing of hMENAΔv6. Total RNA was extracted from MDA-MB-231 cells using TRIzol reagent (Life Technologies) and 2 μg was used to generate a cDNA library using a first-strand cDNA synthesis kit (Amersham Pharmacia Biotech). cDNA was amplified by PCR using hMENA-specific P1-ATG and P8-stop primers as already reported (1). PCR products were analyzed on a 1% agarose gel, excised from the gel, and purified using a gel extraction kit (Qiagen). The extracted amplicon was incubated with 1 unit of AmpliTaq polymerase and 1 μL of 10 mM dATP (both from Applied Biosystems) to add 3′ adenines, and was then cloned into pcDNA3.1/V5-HIS TOPO following the manufacturer's protocol (Invitrogen). Plasmid DNA was isolated by Wizard Plus minipreps DNA purification system (Promega) and was sequenced using T7, T3, and internal sequencing primers for hMena (1).

Cell Lines. The following cell lines were purchased from the American Type Culture Collection: MDA-MB-468, MDA-MB-361, T47D, SKBr3, MCF7, BT474, MDA-MB-231, and BT549 (breast cancer) and SiHa and C33A (cervix cancer); SBT and DAL were developed in our laboratory from the ascitic fluid of two breast cancer patients (2). Cells were cultured in RPMI 1640 (Gibco, Invitrogen) supplemented with 10% (vol/vol) FBS, glutamine, at 37 °C in 5% CO_2 95% air.

Antibody Production. The anti-hMena antibodies used in the present work are described in Fig. 2*A*. A mouse monoclonal antibody (IgG1) specific for the hMENA^{11a} isoform was developed against a 18-aa peptide (RDSPRKNQIVFDNRSYDS) belonging to the 11a exon, purified, and used for WB, immunohistochemistry, and confocal analysis. To obtain antibodies specific to the hMENAΔv6 isoform, rabbits were immunized with a peptide encoded by a region covering the 5 and 7 exon junction (NH2-ERRISSAGIVLG-COOH). The rabbit antiserum was then purified by two-step affinity chromatography using peptides encoded by the 5 and 6 exon junction or by the 6 and 7 exon junction (EWERERRISSAAA and SQQGIVLGPLAPP) to deplete the serum from the antibodies recognizing regions common to all of the hMENA isoforms. The specific IgGs were then purified using the immunogenic peptide (ERRISSAGIVLG) by affinity chromatography. The specificity of the antibodies obtained was evaluated by Western blot on MCF7 (hMENA^{11a}-positive hMENAΔv6-negative), MDA-MB-231 and BT549 (hMENA^{11a}-negative, hMENAΔv6-positive) cells as well as on DAL cells transfected with *hMENA^{11a}*, *hMENAΔv6*, or with the empty vector. The specificity of the hMENA^{11a} Ab immunohistochemical staining was demonstrated by the abolishment of the Ab staining following the preincubation with the immunogenic peptide.The anti-hMENAΔv6 antibody is not suitable for immunofluorescence and immunohistochemistry staining.

RNA Extraction and RT-PCR Analysis. Two micrograms of total RNA, extracted using TRIzol reagent (Invitrogen) were used to obtain the relative cDNA by first-strand cDNA synthesis kit (GE Healthcare). cDNA was amplified using Platinum Pfx DNA polymerase (Invitrogen) in PCR reactions consisting of 35 cycles using MTC1 forward (5′-GCTGGAATGGGAGAGAGAGCGCAGAATA-TC-3′) and MTC4 reverse (5′-GTCAAGTCCTTCCGTCTG-GACTCCATTGGC-3′) primers to detect in the same reaction inclusion or skipping of exons 11a and 6 (Fig. 1*D*). RT-PCR experiments shown in Fig. 4*B* and Figs. S2*B* and S4*B* were performed either with primers P7 forward (5′-GAATTGCTGAA-AAGGGATC-3′) and P8 reverse (5′ CTGTTCCTCTATGCA-GTATTTGAC- 3′) flanking the exon 11a to detect the inclusion/skipping of exon 11a or with primers MTC1 forward and MTC2 reverse (5′-GTTCACACCAATAGCATTCCCTCCACTTG-3′) flanking exon 6. As positive controls, PCR experiments were also done on the pcDNA3.1 vectors containing the *hMENA^{11a}* or *hMENA* variants with P7 forward and P8 reverse primers or on vectors containing *hMENA* and *hMENAΔv6* when using MTC1 forward and MTC2 reverse primers.

PCR products were analyzed on a 1% agarose gel electrophoresis and ethidium bromide staining.

In Vitro Transcription-Coupled Translation. The in vitro translation of *hMENA^{11a}*, *hMENA*, and *hMENAΔv6* cDNA (inserted into the pcDNA3.1 vector) was examined in an in vitro transcription-coupled translation system following the manufacturer's instructions (TNT Rabbit Reticulocyte Lysate System; Promega).

Transfections, Small-Interfering RNA Treatment, and ESRP1 Infection. Cells in exponential growth phase were plated in six-well plates at a density of 3×10^5 cells/well. After 24 h, cells were transfected with 1.5 μg/mL *hMENA^{11a}*, *hMENAΔv6* cDNA, or with vector alone (pcDNA3) or with 100 nmol/L *hMENA*-specific pooled siRNA duplexes (siENA SMART pool) or control nonspecific siRNA (Dharmacon) using Lipofectamine 2000 reagent (Invitrogen), according to the protocol of the manufacturer. Stable transfectants were obtained by selecting transfected cells with 500 μg/mL of G418 (Invitrogen) in culture medium. 293T cells were transfected in T25 flasks with 5 μg of the pMXs-IRES-blast2 Esrp1-FF and pMXs-IRES-blast2 retroviral expression vectors, 1.25 μg of pCMV-VSV-G and 3.25 μg of Gag-Pol using Lipofectamine 2000. After 5 h, the medium was replaced with fresh DMEM with 5% (vol/vol) FBS, and conditioned medium was collected after an additional 24 h. Target cells were transduced with a 50/50 mix of viral supernatant and growth media. Selection was carried out using 10 μg/mL blasticidin.

Western Blot Analysis. Cells were lysed as reported (1). Lysates (30 μg or 50 μg) were resolved on 10% (vol/vol) polyacrylamide gel and transferred to nitrocellulose membrane as described (1). Blots were probed with the following antibodies: 10 μg/mL of pan-hMENA rabbit CKLK1 antibody (1); anti-hMENA^{11a} (0.5 μg/mL) and anti-hMENAΔv6 (0.6 μg/mL); mouse anti–E-cadherin from BD Biosciences; mouse anti–N-cadherin from DakoCytomation in 3% (wt/vol) skimmed milk/TBST overnight at 4 °C. For actin signal, blots were reprobed with monoclonal anti-actin, mouse ascites fluid clone AC-40 (Sigma-Aldrich). Western blot analysis was also performed on 5 μL of in vitro translated hMENA^{11a}, hMENA, and hMENAΔv6.

Wound-Healing Assay. Stably transfected cells were grown to confluence in six-well plates and then scratched. The cells were photographed after 24 and 48 h using an inverted microscope and the size of the wounds was analyzed with ImageJ 1.43 software. Each experiment was performed in triplicate and repeated at least three times.

Cell Invasion Assay. Forty-eight hours after transfection, cells were counted and equal numbers were seeded in Matrigel invasion chamber (24 wells; BD Biocoat Matrigel invasion chamber; BD Biosciences) in duplicate following the manufacturer's instructions. An equal number of stably transfected or control cells (50,000 or 35,000 MDA-MB-231 and BT549; 75,000 MCF7, and 75,000 or

150,000 DAL) were seeded in Matrigel invasion chamber. Cells were allowed to invade for 24, 48, or 72 h, and then were stained, photographed, and at least 10 fields were counted. Each experiment was performed three times.

Three-Dimensional Cultures. HMT-3522 cell lines (S1, S2, and T4-2) were cultured in conventional tissue culture polystyrene and in 3D assays using growth factor reduced reconstituted basement membrane (Matrigel; BD), according to previously described methods (4, 5). Briefly, S2 and T4-2 cells were maintained on flasks coated with acid extracted collagen type I (PureCol; Advanced BioMatrix), whereas for 3D assays, cells were cultured on a thin layer of polymerized Matrigel for 4 d in the presence of growth media containing 5% (vol/vol) lrECM or pharmacological inhibitors. For growth factor depletion, EGF was removed from S1 cultures 24 h before extraction from lrECM. Each lot of pharmacological inhibitors and lrECM used in the study were carefully validated before use in experiments.

Two- and Three-Dimensional Immunofluorescence. For studies in 2D monolayer, cells were cultured in four-well chamber slides (VWR) that were precoated with acid extracted collagen type I (PureCol; Advanced BioMatrix), whereas for 3D studies, cells were cultured in individual wells of a 24-well plate. Cells were fixed in modified paraformaldehyde fixative [60 mM Pipes, 25 mM Hepes, 10 mM EGTA, 2 mM $MgCl_2$, 120 mM sucrose, 4% (wt/vol) paraformaldehyde, final pH 7.4] for either 15 min at room temperature (2D cultures) or simultaneously fixed and extracted from lrECM overnight at 4 °C (3D cultures). For 2D, cells were incubated with pan-MENA mAb (kindly provided by F. Gertler, Massachusetts Institute of Technology, Cambridge, MA) and with hMENA^{11a} mAb according to standard protocols, and were stained using Alexa Fluor 568-phalloidin, Alexa Fluor 488-conjugated donkey antimouse antibody, and DAPI (Invitrogen). For 3D, cell aggregates were stained in suspension using Alexa Fluor 568-phalloidin and DAPI (Invitrogen) and then were streaked on slides and mounted in Vectashield hard set media (Vector Laboratories).

Confocal Microscopy and Image Analysis. Fixed and stained cells were imaged using a Zeiss 710 laser-scanning microscope under 63× Plan Apochromat (1.4 numeric aperture) oil immersion lens with Zen 2008 imaging software (Zeiss). Sequential imaging was used to prevent channel cross-talk in dual-stained samples. For 3D cultures, stacks encompassing the entire volume of colonies were collected in 0.5-μm *Z*-section increments, which were either summarized as a maximum intensity projection (Fig. 4) or rendered into a tomographic representation (Movies S1, S2, S3, and S4), using Imaris software (version 6.1.3; Bitplane).

Patients and Tissue Specimens. A series of 162 patients with breast cancer of different histotypes, surgically treated at the Regina Elena National Cancer Institute (Rome, Italy) between 2000 and 2004, were randomly selected for immunohistochemical studies with informed consent of the patients. Clinicopathologic information of patients with invasive breast cancer is listed in Table S1.

Immunohistochemistry. Pan-hMENA monoclonal antibody (mAb clone 21; BD Transduction) that specifically recognizes all of the hMENA isoforms, was used as previously reported (6). hMENA^{11a} was revealed using the anti-hMENA^{11a}–specific mAb described above. The Novocastra antiestrogen (ER) (6F11 mAb) and progesterone (PgR) (1A6 mAb) receptors were purchased from Novocastra; HER2 (A0485 pAb), Ki67 (MIB-1 MAb), and vimentin (V9 mAb) antibodies were purchased from Dako and E-cadherin from BD Transduction (36-E mAb). Immunostaining was revealed by a streptavidin-biotin enhanced immunoperoxidase technique (Super Sensitive MultiLink; Menarini) in an automated autostainer. Diaminobenzidine was used as chromogenic substrate.

ER and PgR were considered positive when >10% of the neoplastic cells showed distinct nuclear immunoreactivity. Ki67 percentage, based on the median value of our series, was regarded as high if >15% of the cell nuclei were immunostained.

HER2 immunostaining, performed following the manufacturer's protocol, was scored as 0, 1+, 2+, and 3+. Silver in situ hybridization (SISH) (Roche Tissue Diagnostic), was used to determine HER2 amplification in breast cancer defined as equivocal by IHC (score 2+). Therefore, for statistical analysis, negative (score 0, 1+ and IHC 2+ cases lacking amplification) and positive (IHC 2+ amplified cases and Dako score 3+) groups were created. The E-cadherin expression level in breast cancer cells was determined in comparison with normal breast glandular structures present in the peritumoral tissue and scored as normal, reduced, or absent. Normal staining was defined when ≥70% of the tumor cells presented a strong membranous staining, whereas reduced expression was defined when <70% of tumor cells presented a weak membranous staining. No stained cells were observed in the negative cases.

An independent, blinded evaluation of the immunohistochemical results was carried out by two investigators (M.M. and L.P.).

Statistical Analysis. All experiments were repeated a minimum of three times. The data presented in some figures are from a representative experiment, which was qualitatively similar in the replicate experiments. Statistical significance was determined by Student's *t* test (two tailed) comparison between two groups of datasets. Asterisks indicate significant differences of experimental groups compared with the corresponding control condition ($P < 0.05$, see legends of Figs. 3 and 4 and Fig. S3). Statistical analysis was performed using GraphPad Prism 4, V4.03 software.

To assess the relationship between categorical variables, a χ^2 test and Fisher's exact text were used when appropriate. A *P* value of <0.05 was considered statistically significant. All of the analyses were conducted by SPSS 18.0.

1. Di Modugno F, et al. (2007) Molecular cloning of hMena (ENAH) and its splice variant hMena^{+11a}: Epidermal growth factor increases their expression and stimulates hMena^{+11a} phosphorylation in breast cancer cell lines. *Cancer Res* 67:2657–2665.
2. Nisticò P, et al. (1994) Generation and characterization of two human alpha/beta T cell clones. Recognizing autologous breast tumor cells through an HLA- and TCR/CD3-independent pathway. *J Clin Invest* 94:1426–1431.
3. Lee GY, Kenny PA, Lee EH, Bissell MJ (2007) Three-dimensional culture models of normal and malignant breast epithelial cells. *Nat Methods* 4:359–365.
4. Weaver VM, et al. (1997) Reversion of the malignant phenotype of human breast cells in three-dimensional culture and in vivo by integrin blocking antibodies. *J Cell Biol* 137: 231–245.
5. Di Modugno F, et al. (2006) The cytoskeleton regulatory protein hMena (ENAH) is overexpressed in human benign breast lesions with high risk of transformation and human epidermal growth factor receptor-2-positive/hormonal receptor-negative tumors. *Clin Cancer Res* 12:1470–1478.

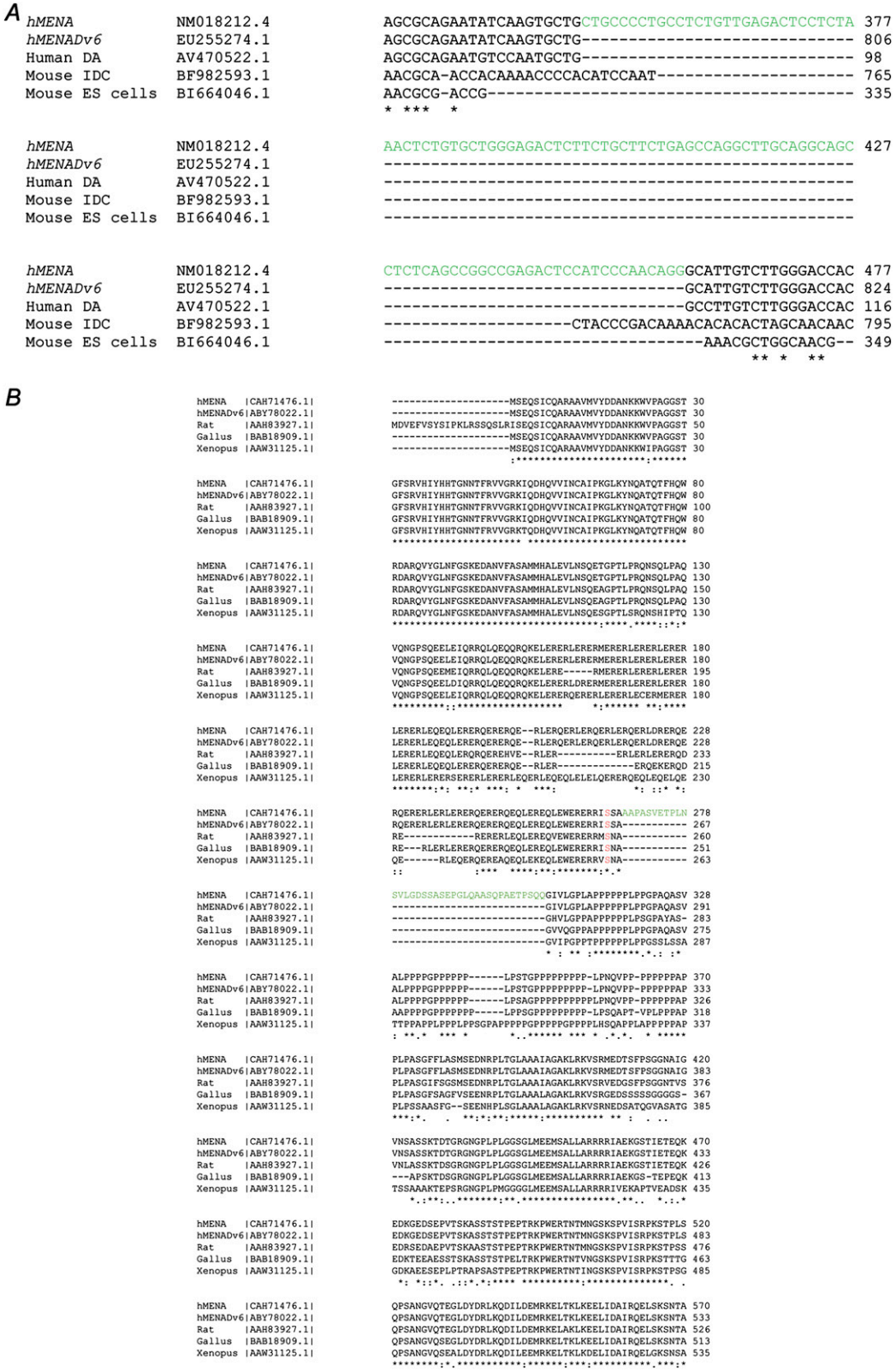

Fig. S1. Molecular cloning and characterization of a unique hMENA splice variant. (*A*) Alignment of *hMENA*, *hMENAΔv6*, human and mouse *ENAH* (*hMENA*) EST nucleotide sequences covering exon 6, which is reported in green (DA, duodenal adenocarcinoma; IDC, mammary infiltrating ductal carcinoma; ES, embryonic stem cells). (*B*) Alignment of human hMENA, hMENAΔv6, and ENAH of *Rattus norvegicus*, AVENAII from *Gallus gallus*, ENABLED of *Xenopus laevis*. Protein sequences were perfomed by ClustalW (exon 6 encoded peptide reported in green).

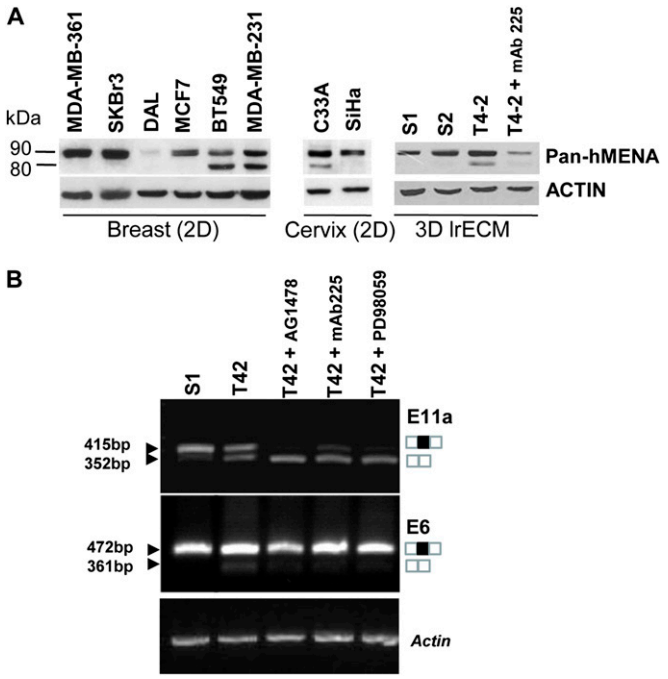

Fig. S2. Analysis of hMENA isoforms, by Western blot with pan-hMENA Ab and hMENA splice variants by RT-PCR in a panel of cell lines. (*A*) Western blot analysis of a panel of 2D growth breast and cervix cancer cell lines and of the 3D-lrECM growth HMT-3522-S1-T4-2 progression series with pan-hMENA CKLK1 Ab reacting with hMENA^{11a} (90 kDa), hMENA (88 kDa), and hMENAΔv6 (80 kDa), indicating that the hMENA isoform is always expressed with either hMENA^{11a} or hMENAΔv6. The hMENA and hMENA^{11a} isoforms are not clearly distinguishable because they comigrate, althought in MCF7 cell lysate, a double band is detectable. Overlapping results were obtained with the pan-hMENA monoclonal antibody (mAb clone 21, BD Transduction). (*B*) *hMENA* transcripts expression in a 3D model of breast cancer progression. RT-PCR analysis of RNA extracted from 3D-grown HMT-3522 S1 (cultured with EGF in the medium), T4-2 cells, and T4-2 cells reverted with AG1478, mAb225, and PD98059 treatments, showing a strong reduction of *hMENA^{11a}* as well as of *hMENAΔv6* splice variants expression following the reversion of the transformed phenotype. RT-PCR experiments were performed either with primers P7 forward and P8 reverse (*Top*) flanking the exon 11a or with primers MTC1 forward and MTC2 reverse flanking exon 6 (*Middle*). RT-PCR with primers specific for β-actin was performed as control of normalization (*Bottom*). PCR products were analyzed by agarose gel electrophoresis and ethidium bromide staining. Length of the amplified products are reported on the *Left*. E6, exon 6; E11a, exon 11a.

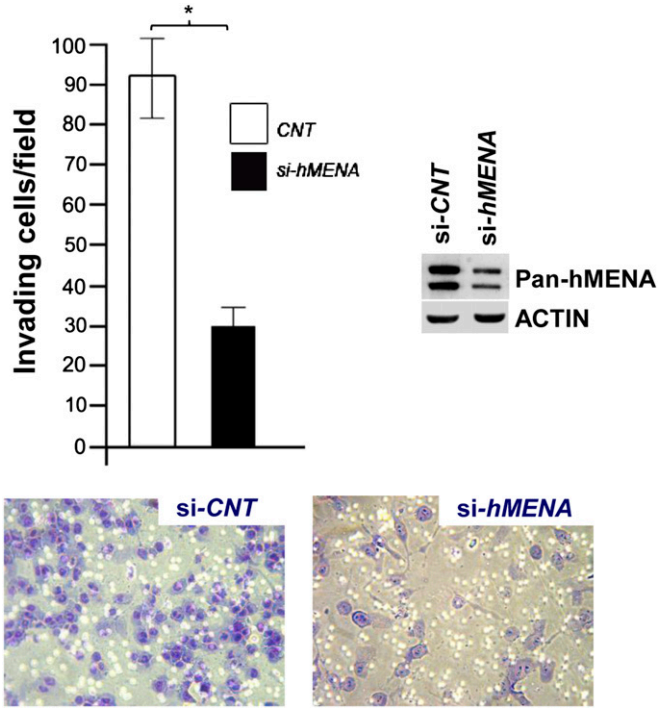

Fig. S3. Pan-hMENA siRNA reduces the invasiveness of BT549 breast cancer cell line. Matrigel invasion assay performed on BT549 cells transfected with the pan-hMENA siRNA (si-*hMENA*), which silences all of the *hMENA* transcripts. The ability of invasion was measured during the last 24 h of transfection using Matrigel-coated transwell filters (BD Biosciences) toward serum. The assay was repeated three times and performed in triplicate each time. Representative images are shown. (*Inset*) Western blot analysis of lysates of BT549 cells collected following 72 h of siRNA transfection.

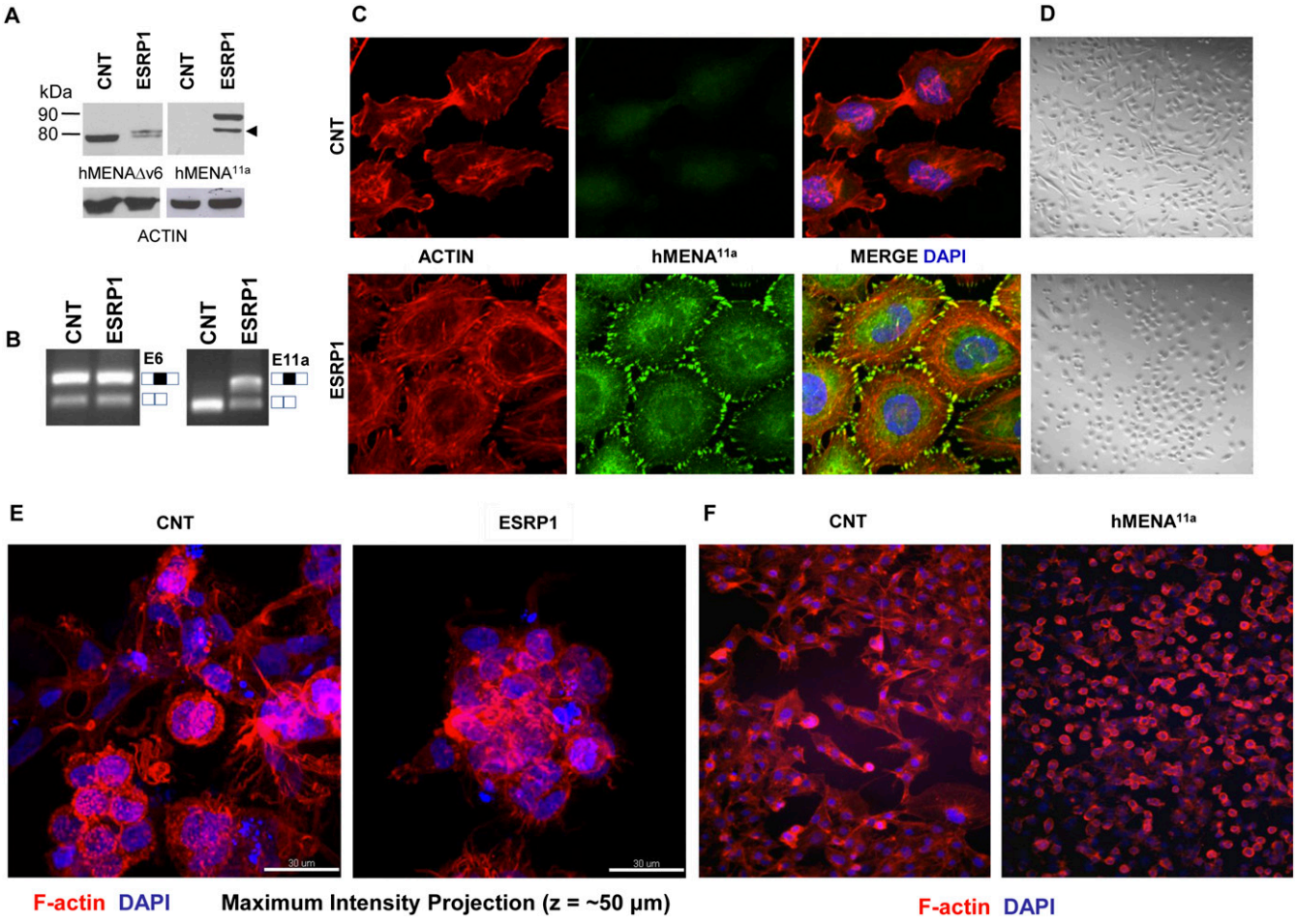

Fig. S4. Epithelial Splicing Regulatory Protein 1 (*ESRP1*) and hMENA^{11a} transfection induce changes in cell shape and actin cytoskeleton architecture in BT549 cells. (*A*) Western blot analysis of BT549 cells transfected with the empty vector (CNT) or with *ESRP1*, with the hMENA isoform-specific antibodies. hMENA^{11a} (90 kDa) is not expressed in the BT549 (CNT) and is induced by *ESRP1* transduction. *ESRP1* also includes the 21 aa of the exon 11a in the hMENAΔv6 isoform (arrowhead), as evident either in the immunoblot with the anti-hMENA^{11a} or with the anti-hMENAΔv6 Abs. (*B*) RT-PCR with RNA extracted from BT549 cells transfected with the empty vector as control (CNT) or with *ESRP1*, performed either with primers flanking exon 6 (*Left*), exon 6 inclusion = □■□; exon 6 skipping = □□, or with primers flanking exon 11a (*Right*), exon 11a inclusion = □■□; 11a skipping = □□. PCR products were analyzed by agarose gel electrophoresis and ethidium bromide staining. E6, exon 6; E11a, exon 11a. (*C*) Confocal analysis of BT549 cells transduced with the empty vector or with ESRP1, by using hMENA^{11a} mAb (green) and phalloidin (red). Cells were imaged using a Zeiss 710 laser-scanning microscope. Magnification, 63×. (*D*) Phase-contrast images of BT549 cells transduced with the empty vector or with *ESRP1*. (*E*) Phalloidin staining of BT549 cells transduced with the empty vector or with *ESRP1* grown in 3D lrECM culture. (*F*) Phalloidin staining of BT549 cells transfected with the empty vector or with *hMENA^{11a}*. Magnification, 20×.

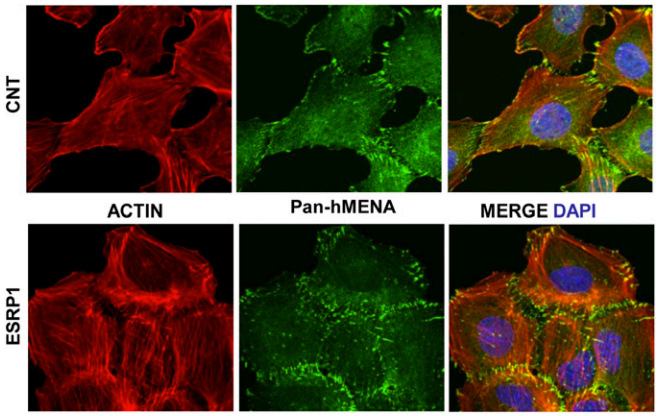

Fig. S5. Confocal analysis of MDA-MB-231 cells transfected with the empty vector or with *ESRP1*. Confocal analysis of MDA-MB-231 cells transduced with the empty vector or with *ESRP1* stained with a pan-hMENA mAb (green) and phalloidin (red). Cells were imaged using a Zeiss 710 laser-scanning microscope. Magnification, 63×.

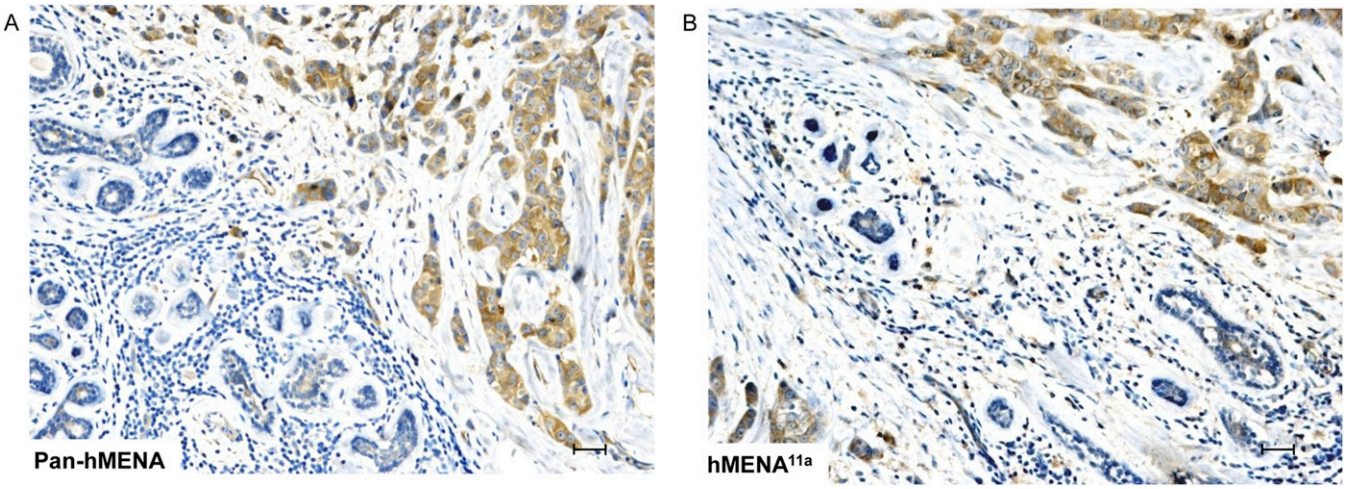

Fig. S6. Immunoreactivity of pan-hMENA and hMENA^{11a} Abs in a representative case of invasive ductal carcinoma. (*A* and *B*) Strong positive immunoreactivity with both pan-hMENA and hMENA^{11a} Abs is evident in tumor cells. Normal ducts surrounding the tumor do not show any immunostaining. Infiltrating lymphocytes are negative. Magnification, 20×. (Scale bars, 30 μm.)

Table S1. Correlation between patients' characteristics and pan-hMENA and hMENA^{11a} staining in 162 primary breast tumors

	Pan-hMENA/hMENA^{11a} staining								
	Pan(–) 11a(–)		Pan(+) 11a(+)		Pan(+) 11a(–)		Total		
Characteristic	No.	%	No.	%	No.	%	No.	%	*P*
	52	32	41	25	69	43	162		
Age, y									0.113
Median range	54		50		57		55		
	32–77		34–75		28–86		28–86		
Histotype									0.121
IDC*	46	88	40	98	65	94	151	93	
ILC†	1	2	0	0	3	4	4	2	
Other	5	10	1	2	1	2	7	5	
Lymph node status									0.527
Negative	32	62	26	63	37	54	95	59	
Positive	20	38	15	37	32	46	67	41	
Tumor size									0.612
T1	37	71	25	61	45	65	107	66	
T2	9	17	11	27	19	28	39	24	
T3 + T4	6	12	5	12	5	7	16	10	
Grade									**0.004**
G1	13	27	5	12	4	6	22	14	
G2	25	51	18	44	46	68	89	56	
G3	11	22	18	44	18	26	47	30	
ER									0.174
Negative (≤10%)	8	15	13	32	17	25	38	23	
Positive	44	85	28	68	52	75	124	77	
PgR									**0.017**
Negative (≤10%)	12	23	21	51	23	33	56	35	
Positive	40	77	20	49	46	67	106	65	
HER2									0.156
Negative (0–1)	47	90	31	76	58	84	136	84	
Positive (2–3)	5	10	10	24	11	16	26	16	
Ki67									**0.0001**
Negative (≤5%)	40	77	15	37	42	61	97	60	
Positive (>15%)	12	23	26	63	27	39	65	40	
E-Cadherin‡									**0.045**
Normal	22	43	18	44	16	24	56	35	
Negative or reduced	29	57	23	56	50	76	102	65	

No., number of patients. $P < 0.05$ reported in bold.
*Infiltrating ductal carcinoma.
†Infitrating lobular carcinoma.
‡Evaluated in nonlobular carcinoma.

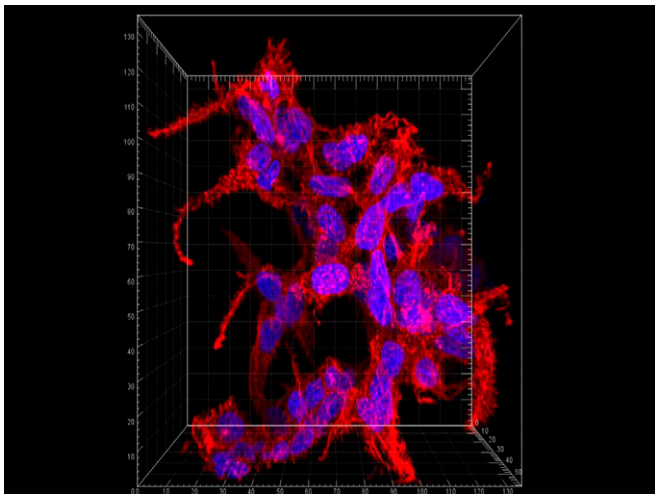

Movie S1. Tomographic projection of MDA-MB-231 control cells cultured in 3D lrECM. Cells were simultaneously fixed and extracted from lrECM using 4% paraformaldehyde buffer containing 10 mM EGTA, then stained in suspension with phalloidin (red) and DAPI (blue). A stack encompassing the entire colony volume was collected in 0.5-μm *Z*-section increments using a Zeiss 710 laser-scanning microscope; the data were then rendered into a tomographic representation using Imaris software (version 6.1.3; Bitplane). *X*, *Y*, and *Z* coordinates (in micrometers) are as indicated.

Movie S1

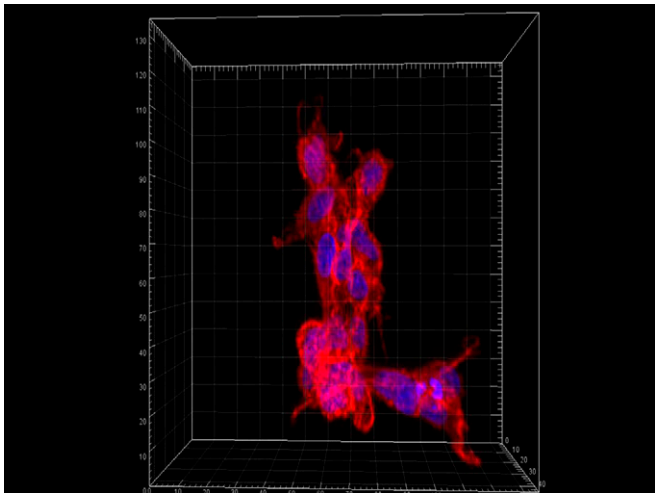

Movie S2. Tomographic projection of MDA-MB-231 ESRP1 cells cultured in 3D lrECM. Cells were simultaneously fixed and extracted from lrECM using 4% paraformaldehyde buffer containing 10 mM EGTA, then stained in suspension with phalloidin (red) and DAPI (blue). A stack encompassing the entire colony volume was collected in 0.5-μm *Z*-section increments using a Zeiss 710 laser-scanning microscope; the data were then rendered into a tomographic representation using Imaris software (version 6.1.3; Bitplane). *X*, *Y*, and *Z* coordinates (in micrometers) are as indicated.

Movie S2

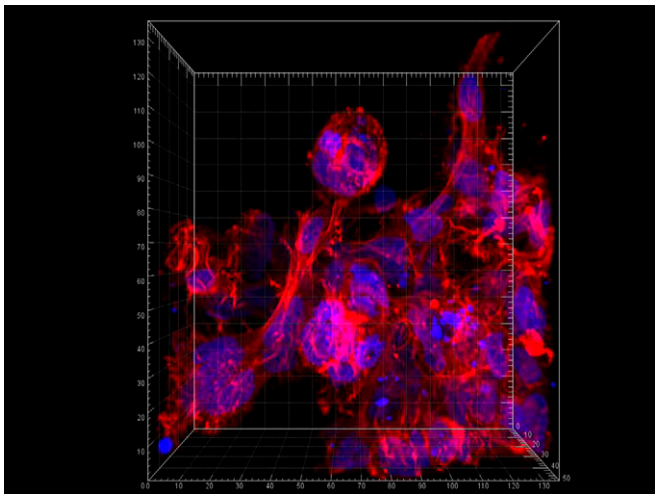

Movie S3. Tomographic projection of BT549 control cells cultured in 3D lrECM. Cells were simultaneously fixed and extracted from lrECM using 4% paraformaldehyde buffer containing 10 mM EGTA, then stained in suspension with phalloidin (red) and DAPI (blue). A stack encompassing the entire colony volume was collected in 0.5-μm *Z*-section increments using a Zeiss 710 laser-scanning microscope; the data were then rendered into a tomographic representation using Imaris software (version 6.1.3; Bitplane). *X*, *Y*, and *Z* coordinates (in micrometers) are as indicated.

Movie S3

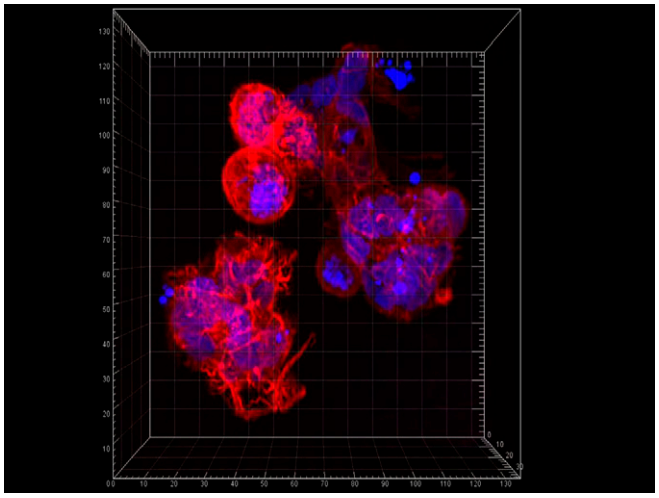

Movie S4. Tomographic projection of BT549 ESRP1 cells cultured in 3D lrECM. Cells were simultaneously fixed and extracted from lrECM using 4% paraformaldehyde buffer containing 10 mM EGTA, then stained in suspension with phalloidin (red) and DAPI (blue). A stack encompassing the entire colony volume was collected in 0.5-μm *Z*-section increments using a Zeiss 710 laser-scanning microscope; the data were then rendered into a tomographic representation using Imaris software (version 6.1.3; Bitplane). *X*, *Y*, and *Z* coordinates (in micrometers) are as indicated.

Movie S4